A new rheometer for paper coating

Akira Tsuji, Junichiro Nitta, Yasuhiko Sasagawa, and Norichika Nojima

A new instrument, the Slit Die Rheometer, measures the viscosity and flow behavior of coating colors at a very high shear rate, simulating the coating flow beneath the blade tip in the actual blade coating process.

As paper coating technology advances, coating rheology at high shear rates is being studied as a way to estimate the coating's runnability and to understand what happens in the coating process. On modern blade coating machines, the coating color is sheared at over 10^6 s^{-1} beneath the blade at a coating speed of more than 1000 m/min. The capillary viscometer is reported to be a useful apparatus for studying such high shear rheology, because it can measure the viscosity up to around 10^6 s^{-1} (*1, 2*). Recently, Ramthun *et al.* proposed an interesting device that can measure the viscosity at greater than 10^6 s^{-1} (*3*).

Another new rheometer, called the "slit die rheometer" (SDR), is presented here. The SDR can give an accurate measurement of the rheological properties at the high shear rate of more than 10^6 s^{-1}, a rate that is relevant to runnability in high-speed blade coating.

Design of the SDR

The design of the SDR is illustrated in **Fig. 1**. The sample is extruded from a reservoir through a slit die by a piston driven at a steady and constant speed with a servomotor. Two kinds of slit dies (Slit A and Slit B) are available; these have the same width w, but they vary in thickness h and length L. Slit A is equipped with three pressure transducers along the slit flow channel and is attached to a reservoir 30 mm in diameter. Slit B, with one pressure transducer, is attached to a reservoir 20 mm in diameter.

The maximum speed (5 m/min) of the piston with the maximum loading force of 30 kN can generate high flow rates in the slit dies: 1414 m/min for Slit A and 1571 m/min for Slit B. A stepwise change of piston speed can cover the high shear rheology at 2×10^4 s^{-1} to about 6×10^5 s^{-1} for Slit A and 5×10^4 s^{-1} to about 2×10^6 s^{-1} for Slit B.

The first pressure transducer, P1, is located as near the entrance as possible so that we may study the turbulent flow at the entrance of the slit. This behavior is expected to simulate the turbulence at the entrance of the blade in the actual coating process. The viscosity of the steady flow can be obtained accurately without any correction by using the difference of the pressure at P2 and P3 for Slit A. Slit B is equipped with only one pressure transducer, P1, because of its thickness and length, which is necessary in order to obtain the high shear rate of $>10^6$ s^{-1} within the maximum loading force. The viscosity can also be obtained for Slit B by using the pressure at P1, but it contains some error due to the unsteady behavior at the edge of the slit. The pressure at P1 for Slits A and B can give meaningful information for use in estimating the runnability because it corresponds to the pressure of the coating color against the blade in the actual blade coating process.

Evaluation of the SDR data

Han has made a theoretical study of the slit die rheometer in polymer rheology (*4*). The analysis of the SDR data is based on his study.

Calculations

The shear stress T is calculated as:

$$T = h\Delta P/(2\,len) \quad (1)$$

where

h = thickness

ΔP = the pressure difference between two points on the slit wall

len = the length between points.

The apparent shear rate at the wall, Ra, (assuming the Newtonian flow) has been calculated using:

$$Ra = 6Q/w\,h^2 \quad (2)$$

where

$$Q = V\pi r^2 \quad (3)$$

where

Q = volumetric flow rate

V = the speed of the piston

r = radius of the reservoir.

By applying the Rabinowitsch-Weissenberg correction,

Tsuji is research associate, Nitta is chief chemist, Sasagawa is chief chemist, and Nojima is chemist at Emulsion Laboratory, Technical Center, Japan Synthetic Rubber Co., Ltd., 100 Kawajiri-cho, Yokkaichi 510, Japan.

1. A diagram of the slit die rheometer, showing Slit A and Slit B (For Slit A and Slit B, width w = 10 mm. For Slit A, thickness h = 0.25 mm and length L = 35 mm. For Slit B, h = 0.1 mm and L = 15 mm.)

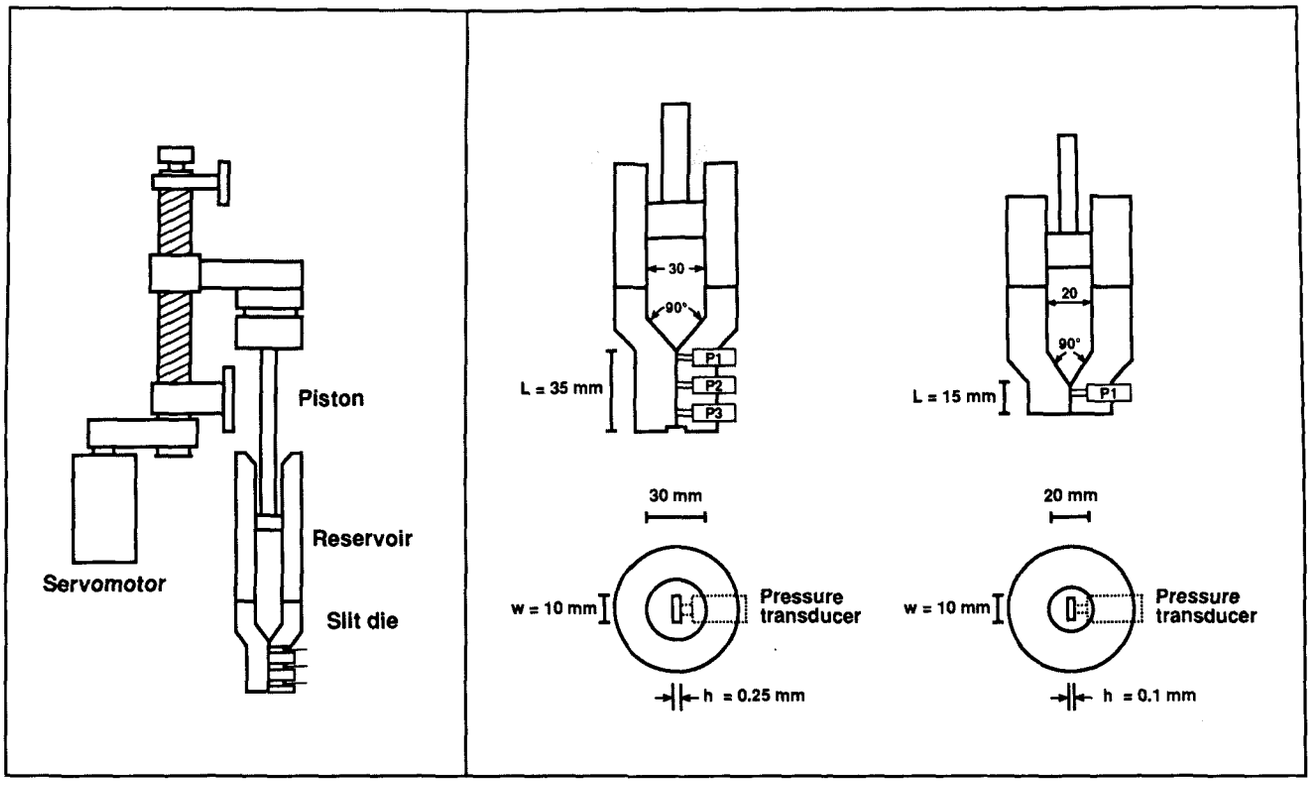

2. Pressure profiles of low-, medium-, and high-viscosity silicone oil at various shear rates for Slit A

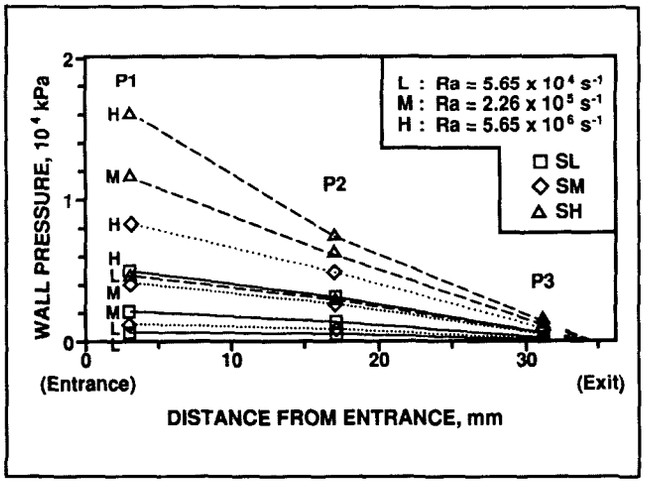

3. Logarithm of shear stress vs. logarithm of apparent shear rate

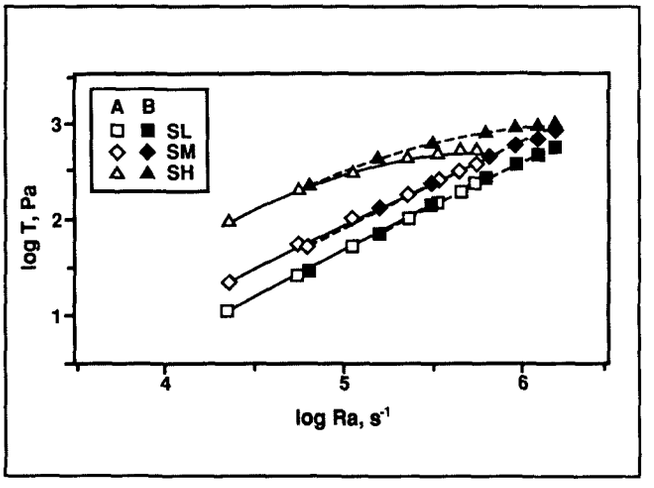

we obtain the true shear rate:

$$R = 1/3\,[2 + (d \log Ra/d \log T)]Ra \quad (4)$$

And the true viscosity N is determined by:

$$N = T/R \quad (5)$$

Example: silicone oil

To clarify the description, let us take the example of measuring three kinds of silicone oil of different viscosities—low (SL), medium (SM), and high (SH). Silicone oil behaves like a Newtonian fluid, and **Fig. 2** shows part of the pressure profiles of silicone oil in using Slit A.

The difference between the slope of (P1 - P2) and that of (P2 - P3) seems to be caused by the effect of some turbulence at the entrance on the pressure at P1, with this being generally known as an edge effect. The difference of the pressure at P2 and P3 is adopted as ΔP to calculate the viscosity of the steady flow for Slit A. That the flow is steady between P2 and P3 can be proved by the fact that the exit pressure determined by extrapolating the wall pressure of P2 and P3 to the exit of the slit is almost zero, as indicated in Fig. 2.

For Slit B, the viscosity can be taken by using the value

4. True viscosity vs. the wall shear rate for low-, medium-, and high-viscosity silicone oil for Slits A and B

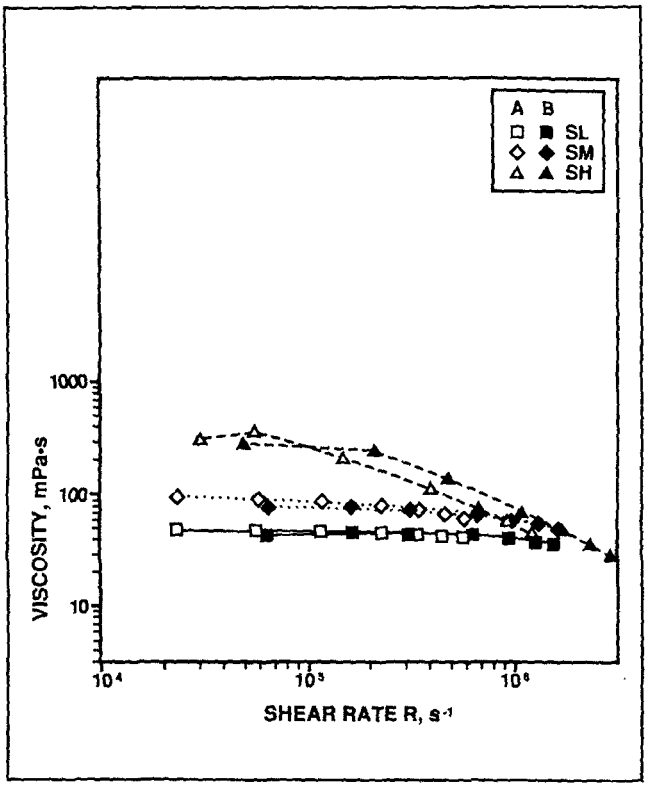

5. Viscosity vs. shear rate for silicone oil for Slits A and B and including the data with the Concentric Cylinder Hi-shear Viscometer (Hi)

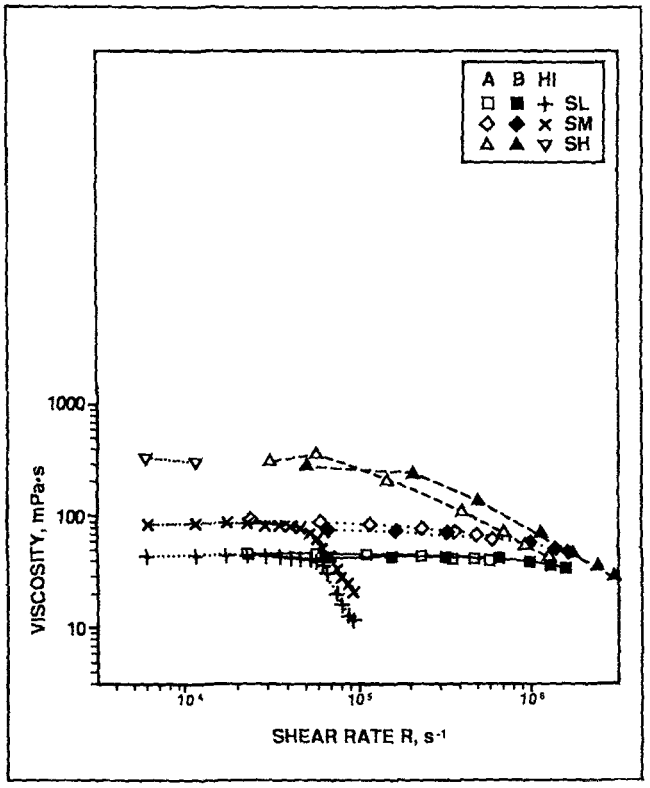

6. Viscosity vs. shear rate for clay slurry (U.S. No. 2 grade)

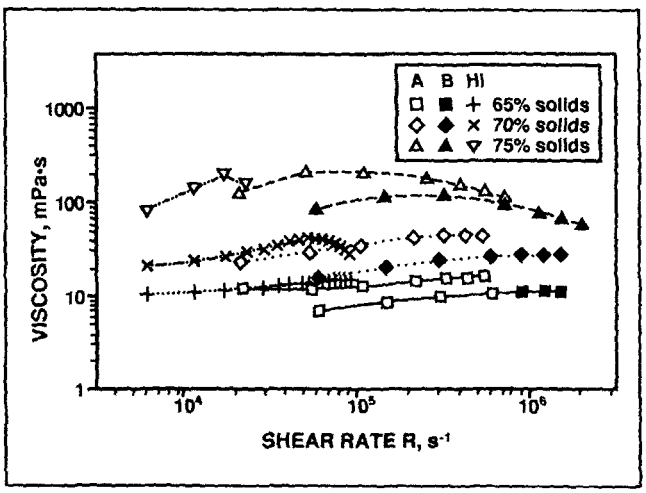

7. Viscosity vs. shear rate for a slurry of fine ground calcium carbonate

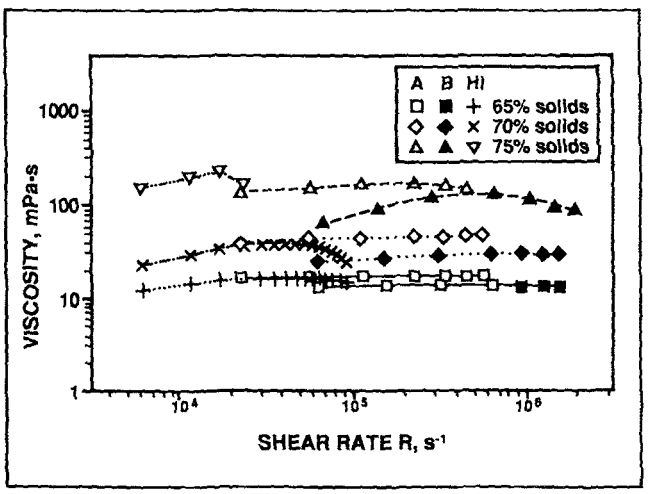

of P1 itself as ΔP, assuming that the pressure at the exit of the slit is equal to 0. However, the value contains some error due to the turbulence at the entrance.

In **Fig. 3**, log T is plotted against log Ra. Straight lines are obtained except for the silicone oil of high viscosity (SH). This result indicates that SL and SM can be treated as a power law fluid in agreement with the following equation:

$$T = K\,Ra^n \tag{6}$$

$$n = [(d \log T)/(d \log Ra)] \tag{7}$$

Whether the sample is a power law fluid or not, n can be calculated by the differentiation of the function of log T to log Ra—that is, the slopes of the plots of log T vs. log Ra as determined by the least squares method. The true viscosity can be given by Eqs. 1, 4, and 5. **Figure 4** shows the true viscosity plotted against the wall shear rate for Slits A and B. Slit A can give an accurate viscosity in the steady state without any more correction. The viscosity for Slit B is almost the same as that for Slit A except in SH, because the degree of turbulence at the entrance seems to be small except in the flow of SH, as shown in Fig. 2. Also, this similarity in viscosity is

8. Viscosity vs. shear rate for a high-solids SB latex for paper coating

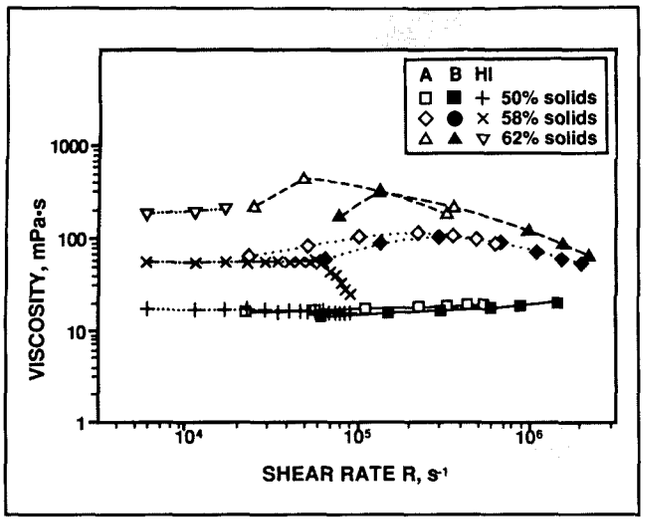

9. Viscosity vs. shear rate for oxidized starch solution

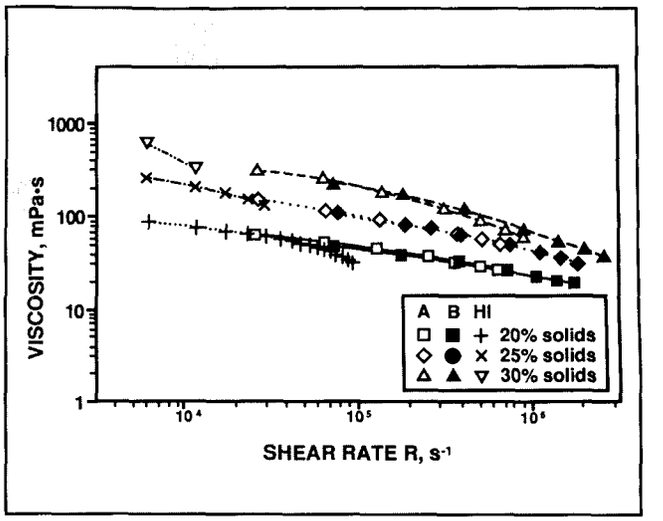

substantiated by the fact that SL and SM behave like a Newtonian fluid at the high shear rate of $>10^6$ s^{-1}.

Comparison with the Concentric Cylinder Hi-shear viscometer

In **Fig. 5**, the data of the apparent viscosity vs. the apparent shear rate determined with the Concentric Cylinder viscometer are added to the data of the SDR. The data in the region of the low shear rate in the Concentric Cylinder viscometer correspond well with the data of the SDR. However, the viscosity in the region of the high shear rate in the Concentric Cylinder viscometer seems to exhibit an extreme shear-thinning behavior, which may be caused by the temperature rising as a result of the repeated mechanical shear during measurement in the Concentric Cylinder viscometer.

Also, the Concentric Cylinder viscometer cannot give the viscosity at a shear rate as high as can the SDR, as a result of its mechanical limitation. Linking the data of the Concentric Cylinder viscometer and that of the SDR can cover the high shear viscosity in the wider region of shear rate.

Examples of measuring materials for paper coating with the SDR

Figures 6-9 present the results of measuring the high shear viscosity with the SDR and the Concentric Cylinder viscometer for:

- Clay slurry
- Ground calcium carbonate slurry
- SB latex
- Starch aqueous solution.

These have various solids contents.

The first three materials of two-phase dispersion exhibit more dilatant behavior and more difference in the viscosity between Slit A and Slit B as the solids contents increase. Especially, clay slurry containing anisotropic particles reveals remarkable dilatancy and difference in the viscosity between Slit A and Slit B. On the other hand, in the case of the starch solution, which shows a typical pseudo-plastic flow, the viscosity for Slit B agrees with that for Slit A, as with the low-viscosity silicone oil.

10. Pressure at P1 vs. shear rate for the clay slurry

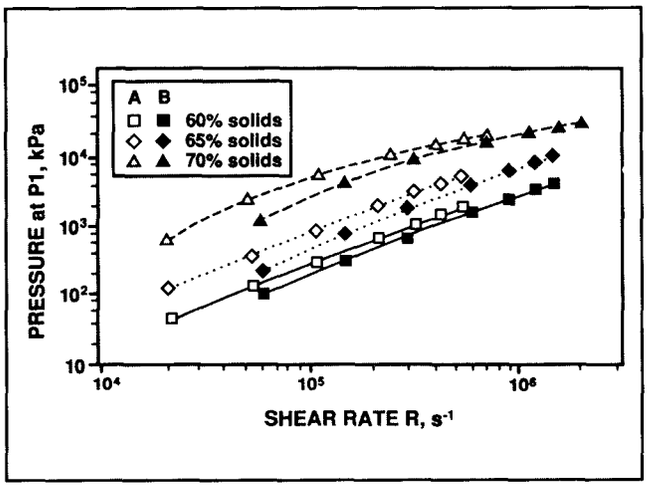

Figures 10 and 11 shows the pressure at P1 plotted against the shear rate for Slits A and B for the clay slurry and the starch solution. Clay slurry gives a large pressure difference at P1 between Slit A and Slit B, but both are the same in the starch solution. The turbulence near the entrance of the slit is increased by the dynamic particle orientation in the dispersion as particles are forced into the narrow slit. The turbulent state is affected by the ease with which particles become oriented, which is a function of the shape of the particles and the width of the slits. Therefore, the difference of the viscosity and the pressure at P1 between Slits A and B reflects the dynamic state of the particle orientation under the high shear rate in the dispersion system. The latex spherical particles become oriented more easily than the irregular stone-like particles of calcium carbonate, and calcium carbonate becomes oriented more easily than clay of plate particles (Figs. 6-8).

11. Pressure at P1 vs. shear rate for the starch solution

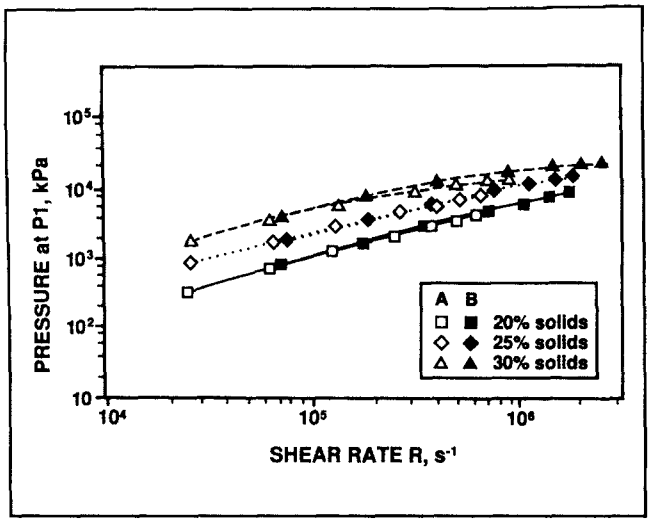

I. Results of the coating trials with the pilot coater

	Color formulation			
	No. 1	No. 2	No. 3	No. 4
Pigment				
U.S. No. 2 clay	100	100	70	70
$CaCO_3$	...	...	30	30
SB latex particle				
Particle size	Medium	Medium	Medium	Small
Parts	14.75	5	12	12
Cobinder				
Type	CMC	Starch	Starch	Starch
Parts	0.25	10	3	3
Solids content, %	65.5	57	64	64
Runnability	Heavy bleeding	Trouble-free	Slightly bleeding	Trouble-free

SB = styrene-butadiene. CMC = carboxymethyl cellulose.

12. Viscosity vs. shear rate for No. 1 and No. 2 coating color

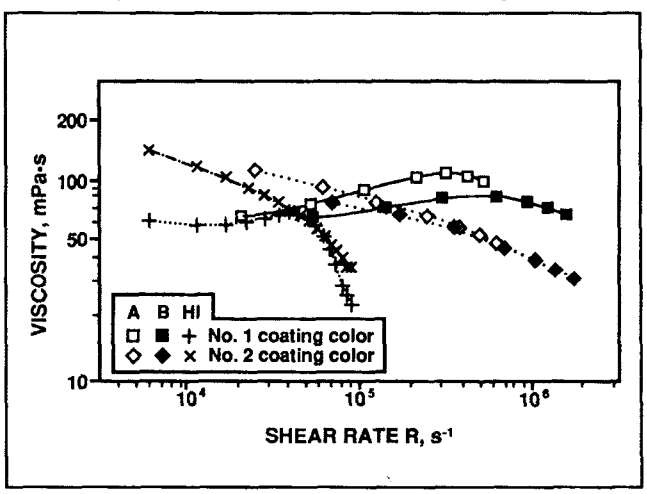

In the viscosity curves, we observe shear-thinning behavior and the reduction of the difference in the viscosity in the region of the higher shear rate. Similarly, in the curves of P1 pressure vs. shear rate in the dispersion samples of high solids content, we observe shear-thinning behavior and the reduction of the difference in P1 pressure for Slits A and B in the region of the higher shear rate. This may suggest that the reduced particle concentration caused by the shear-induced phase separation at the wall produces "slippage," which decreases the viscosity and P1 pressure (*5*).

The recent trend of increasing the coating speed and the solids content of the coating color makes it even more important to understand these properties and the part they play in the coating process.

Relationship between runnability and the SDR data

Four different coating colors were applied to a woodfree basesheet of 81 g/m² using the variable-dwell-time blade coater at a speed of 1000 m/min. The color formulation and the results of the coating trials are presented in **Table I.**

For Nos. 1 and 2, the viscosity near 10^5 s^{-1} as measured using the SDR is almost the same, as shown in **Fig. 12.** However, the flow behavior is quite different, as reflected in the differences in runnabilities, which was caused by the difference in the binder system and the solids content. No. 3 is the same formulation as No. 4 except that the kind of latex is different. These formulations exhibit the same flow behavior but a difference in viscosity as measured using the SDR (**Fig. 13**).

Figure 14 shows the heavy bleeding that occurred in the trial with the No. 1 coating color, which exhibited an extreme dilatant flow. The higher viscosity of No. 3 caused a slight bleeding. No. 2 and No. 4 provided good runnability. These results show that the flow behavior and the viscosity at the high shear rate, more than 10^5 s^{-1} as measured using by the SDR, relates to the runnability in the high-speed blade coating. Also, **Fig. 15** demonstrates that the pressure at P1 can be used in estimating the runnability. Although Slit B cannot give as accurate a viscosity of the steady flow as Slit A, it can provide the P1 pressure to more than 10^6 s^{-1}, which is sufficient to estimate the runnability.

Of course, the viscosity and the flow behavior in the steady flow given with Slit A are important in estimating the runnability and understanding what happens in the coating process. However, the pressure at P1 with Slits A and B may be an even more useful information for predicting the runnability because P1 is expected to simulate the unsteady behavior of the coating flow under the thin blade in the actual blade coating process.

Conclusions

The Slit Die Rheometer can measure rheological properties at a very high shear rate (10^4 s^{-1} to $>10^6$ s^{-1}) by measuring the normal stress directly at the wall of the narrow slit when the coating color is extruded through the slit at a high rate of flow. This mechanism of the SDR gives a good simulation to the coating flow beneath the blade tip in the actual blade coating process. The SDR can give not only accurate high shear rheological

properties (the viscosity and the flow behavior in the steady flow) without any correction, but it can also give the pressure at P1, which stimulates the unsteady flow behavior under the blade. Both of these properties relate to the runnability in the high-speed blade coating process.

Finally, the SDR provides interesting observations of the effect of the particle orientation on the unsteady flow behavior at the entrance and the effects of the slippage on the high shear rheology. Such observations can lead to a better understanding of the coating process.□

Literature cited

1. Canard, P., Tappi 57(11): 95(1974).
2. Harsveldt, A., Paper Tech. and Ind. (Jan-Feb):15(1981).
3. Ramthun, J., Wallpot, G., Reif, L., and Rahles, D., 1989 Coating Conference Proceedings, TAPPI PRESS, Atlanta, p. 27.
4. Han, C. D., Rheology in Polymer Processing, Academic Press, New York, 1976, p. 89.
5. Seshadri, V. and Sutera, S. P., Trans. Soc. Rheology 14(3): 351(1970).

Received for review Jan. 25, 1990.

Accepted May 1, 1990.

13. Viscosity vs. shear rate for No. 3 and No. 4 coating color

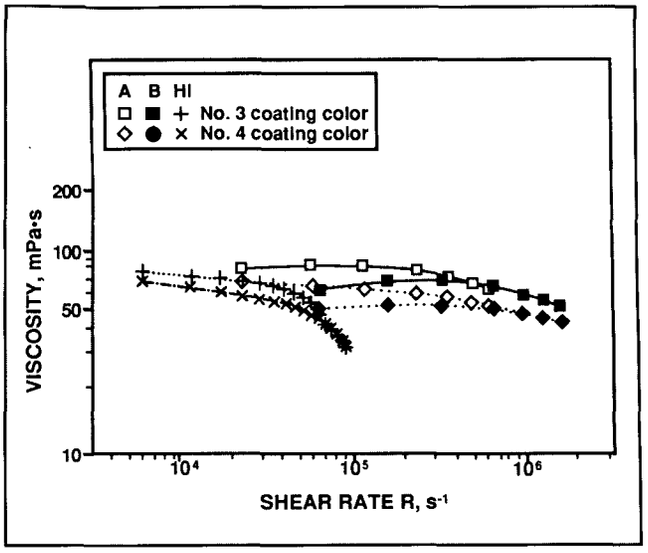

14. Picture of bleeding at the coating trial for No. 1 coating color

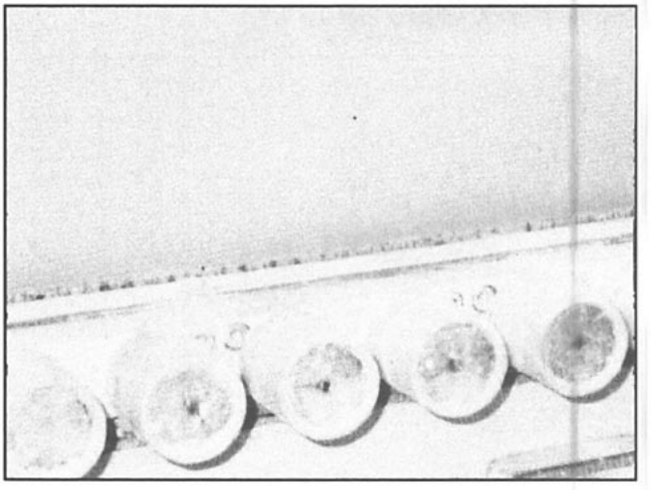

15. Pressure at P1 vs. the shear rate for the coating colors